

Toward a Greener Bioeconomy: Synthesis and Characterization of Lignin–Polylactide Copolymers

Tim Langletzt, Philipp M. Grande, Jörn Viell, Daniel Wolters, Josia Tonn, Holger Klose, Sascha G. Schriever, Alexander Hoffmann, Andreas Jupke, Thomas Gries, and Sonja Herres-Pawlis*

In the modern world, plastics have become indispensable. Due to their properties, they are used for a wide variety of applications ranging from packaging materials to textiles and medical technology. The vast majority of these plastics are made from finite fossil feedstocks that will need to be replaced in the long term to meet consumer demands in the future. Intensive research is being conducted into alternative bio-based feedstocks to replace petroleum-based plastics with more environmentally friendly variants. This includes polylactide, a polyester derived from lactic acid, which is mainly used as packaging material. In this work, star-shaped copolymers consisting of polylactide and OrganoCat lignin with varying lignin loadings are synthesized using a “grafting-from” approach directly from the lactide melt using a zinc-based guanidine catalyst. This method proves to be efficient and copolymers can be produced after 30 min to three hours with high lactide conversions. Kinetic studies are performed to investigate the influence of different lignin loadings on the polymerization rate and ^{31}P NMR experiments are used to analyze the functionalization of the lignin. Thermal analysis reveals an increase of the glass transition temperature and a higher thermal decomposition temperature with increasing lignin content.

properties. Since 1950, the annual production of various types of plastics has been steadily increasing.^[1–3] In 2021, the annual global production of plastics amounted to 390.7 Mt, of which 32.5 Mt originated from recycled material and 5.9 Mt from bio-based feedstocks. While the latter numbers may seem small, their significant annual increase demonstrates more the potential of bio-based plastics.^[4] This trend is accelerated by the depletion of fossil resources and environmental pollution caused by nondegradable plastics.

A promising bio-based and biodegradable plastic is polylactide (PLA).^[5–7] The industrial synthesis of polylactide is carried out by ring-opening polymerization (ROP) of lactide (LA) with tin octanoate ($\text{Sn}(\text{Oct})_2$). Tin octanoate has cytotoxic properties and can accumulate during the biodegradation of PLA, thereby posing a hazard to the environment.^[8–10] For this reason, research is being conducted into alternative, non-

toxic metal-based catalysts for the ROP of lactide.^[11–18] The Herres–Pawlis group recently published robust, nontoxic^[19] guanidine catalysts based on iron^[20] and zinc,^[21,22] which outperform the industrially used tin octanoate and represent a

1. Introduction

Plastics have become an indispensable part of modern life, offering a wide range of applications thanks to their unique

T. Langletzt, A. Hoffmann, S. Herres-Pawlis
Institute of Inorganic Chemistry
RWTH Aachen University
Landoltweg 1a, 52074 Aachen, Germany
E-mail: sonja.herres-pawlis@ac.rwth-aachen.de

T. Langletzt, P. M. Grande, J. Viell, D. Wolters, J. Tonn, H. Klose,
S. G. Schriever, T. Gries, S. Herres-Pawlis
Bioeconomy Science Center (BioSC)
Forschungszentrum Jülich GmbH
52425 Jülich, Germany

P. M. Grande, H. Klose
Institute of Bio- and Geosciences: Plant Sciences
Forschungszentrum Jülich GmbH
Wilhelm-Johnen-Straße, 52428 Jülich, Germany

J. Viell
NGP2 Biorefinery
RWTH Aachen University
Forckenbeckstraße 51, 52074 Aachen, Germany

D. Wolters, S. G. Schriever, T. Gries
Institute of Textile Technology
RWTH Aachen University
Otto-Blumenthal-Straße 1, 52074 Aachen, Germany

J. Tonn, A. Jupke
Fluid Process Engineering (AVT, FVT)
RWTH Aachen University
Forckenbeckstraße 51, 52074 Aachen, Germany

H. Klose
RWTH Aachen University
52074 Aachen, Germany

The ORCID identification number(s) for the author(s) of this article can be found under <https://doi.org/10.1002/aesr.202300187>.

© 2023 The Authors. Advanced Energy and Sustainability Research published by Wiley-VCH GmbH. This is an open access article under the terms of the Creative Commons Attribution License, which permits use, distribution and reproduction in any medium, provided the original work is properly cited.

DOI: 10.1002/aesr.202300187

promising alternative. PLA has several advantageous properties such as biocompatibility, processability, and energy savings during production compared to petroleum-based polymers. Nevertheless, properties such as low toughness, slow degradation rate, hydrophobicity, and lack of reactive side groups pose challenges for its application areas.^[23]

One way to improve the properties of PLA or adapt it to specific applications is to incorporate other polymer chains, resulting in copolymers.^[24] For example, the copolymer of PLA and polycaprolactone (PCL) shows improved toughness and/or elongation at break compared to pure PLA.^[25,26] Furthermore, the incorporation of glycolic acid (GA) into the PLA chain leads to PLGA copolymers, which can be used in biomedical applications for bone tissue engineering. Additionally, the PLGA copolymers show decreased degradation times depending on the monomer ratios.^[27] There are a variety of other PLA copolymers for different applications, the reader is referred to respective literature reviews.^[24,28–33]

Another potential candidate which can be used to generate copolymers with enhanced properties is lignin.^[34,35] After cellulose, it is the second most abundant organic carbon source in the biosphere. It is mainly produced as a byproduct of pulping processes.^[36] Typically it is burned to generate energy for other process units, and only 2% is used as a value-added product, primarily as dispersant, adhesive, or surfactant.^[37] Lignin itself is a complex, 3D macromolecule mainly built of cross-linked phenylpropanoid units, namely, para-coumaryl alcohol (H-type), coniferyl alcohol (G-type), and sinapyl alcohol (S-type). It possesses methoxy, carbonyl, and phenolic, aromatic, as well as carboxylic hydroxyl groups.^[38,39] Its structure and composition depend on multiple factors: the type of plant and tissue, the plant's developmental stage, environmental factors during plant growth, and the specific extraction process.^[40,41] This high variability displays one of the major challenges for an advanced utilization of lignin in industrial applications.^[42] Despite those challenges, there is a growing interest in a higher value utilization for lignin.^[43] Lignin has the potential to provide an environmentally and economically sustainable feedstock for different applications such as fuels, chemicals, and materials.^[37] Moreover, lignin extraction is not in direct competition with the food industry, which is an additional argument in favor of using lignin as a monomer for bio-based plastics.^[36] In recent years, more processes have been developed that focus on the usage of lignin. These so-called lignin-first approaches use processes that extract lignin at mild conditions, resulting in favorable properties of lignin due to less degradation and higher purity of the lignin.^[44] One such process is the OrganoCat process, using phosphoric acid to reactively open up the lignocellulose structure, while extracting lignin into a second 2-methyltetrahydrofuran (MTHF) phase.^[45] Due to the mild reaction conditions, the potential for degradation products is low since few-to-no humins are formed and high lignin linkage content is conserved in the extract.^[45,46]

Since the free hydroxyl groups are an excellent target for functionalization, some lignin-based plastics with improved properties have already been published in the literature. In the presence of copper(I) salts and a N-donor ligand, lignin can be functionalized via atom transfer radical polymerization (ATRP) through a “grafting from” approach. Usually, the hydroxyl groups of lignin are functionalized with 2-bromoisobutyl bromide. The

modified lignin acts as an excellent initiator for acrylate monomers.^[47] In addition, lignin can be used for the synthesis of polyurethane foams, which are traditionally based on petroleum-based feedstocks. Lignin acts here as a polyol monomer, which is converted into the corresponding polyurethane with isocyanates. Compared to its petroleum-based polyol alternative, lignin-based polyurethane foam exhibits higher biodegradability and lower cost, highlighting the potential of lignin application in sustainable materials.^[48] Due to its high carbon content of about

60 %, lignin is a potential substitute for polyacrylonitrile (PAN) as a precursor for carbon fiber production. PAN is obtained from fossil raw materials and its production is relatively cost intensive. Lignin as an alternative could reduce the price and improve the sustainability of the corresponding carbon fibers.^[49] Furthermore, lignin can be functionalized through ROP of different cyclic monomers such as alkylene oxides,^[50–56] ϵ -caprolactone (CL),^[57–64] and lactide.^[65–73] In 2002, Hatakeyama et al. reported the functionalization of Alcell and Kraft lignin via ROP of CL after 12 h at 150 °C in the presence of dibutyltin dilaurate as catalyst. The authors produced polyurethane (PU) sheets from those copolymers through reaction with diphenylmethane diisocyanate at room temperature in THF. Subsequent evaporation of the solvent and curing at 120 °C for two hours yielded the respective PU-sheet. Thermal properties of the material depends on the PCL chain length, which can be controlled through the CL/OH ratio.^[57] Avérous et al. prepared lignin–CL copolymers from soda lignin and CL in bulk or in dry toluene at 130 °C for CL/OH molar ratios from 5 to 100 using $\text{Sn}(\text{Oct})_2$. The reaction proceeded within 14–62 h under anhydrous conditions, to avoid homopolymerization reactions. Interestingly, the authors found that the resulting copolymer with CL/OH ratios of 5 forms an amorphous, flexible material, due to 3D hydrogen bonding networks of the carbonyl group of PCL and phenolic hydroxyl groups. At a CL/OH ratio higher than 5, PCL chains form a semicrystalline structure, leading to PCL/lignin phase segregation, which causes the flexible network to disappear and a brittle material is obtained.^[58] Sattely et al. reported the synthesis of lignin–PLA copolymers directly in the lactide melt at 130 °C in the presence of the organocatalyst triazabicyclodecene (TBD), which yields the copolymer after 3–4 h. The resulting copolymers showed improved mechanical properties as well as improved UV absorbance compared to PLA.^[65] Mehrkhodavandi et al. reported two strategies to generate lignin–PLA copolymers. A multistep synthesis using a “grafting onto” approach starting from the prepolymerization of lactide to yield PLA and a subsequent chlorination of the end groups led to the corresponding PLA–Cl. This could be used to functionalize the hydroxyl groups of lignin under alkaline conditions with lignin contents of 5 wt%. The second possibility was polymerization by an indium-catalyzed ROP of lactide in the presence of triethylamine in toluene at 120 °C over 24 h.^[66] To achieve higher PLA chain segment molecular weights, lignin can be peralkylated prior to polymerization with lactide. Liu et al. presented a green approach for the alkylation of alkaline lignin. Using 1-bromododecane, potassium carbonate, and catalytic amounts of tetrabutylammonium bromide in an aqueous reaction system, an alkylated lignin was obtained after three days in which all phenolic hydroxyl groups and 77% of the carboxylic acid groups were

functionalized. Subsequent reaction of the dodecylated lignin with lactide and catalytic amounts of DBU in anhydrous DCM provided the corresponding copolymer after 24 h, which exhibited PLA chain length segments of more than 10 k Da. The respective PLA/lignin-PLA blend with a chain length of more than 10 k Da showed an improved elongation of more than 200%, corresponding to a 40-fold improvement compared to neat PLA. In addition, tensile strength and Young's modulus were also increased, and the material showed improved UV blocking ability.^[68]

This demonstrates the potential of lignin for use in the plastics sector to improve the properties of bioplastics and adapt them to specific applications, as well as to obtain a value-added product from a material that is currently rather underutilized.

In this work, we could show that OrganoCat lignin-PLA copolymers can be synthesized efficiently with low catalyst loadings using a nontoxic zinc catalyst without the usage of solvents. In order to gain a better understanding of the reaction mechanism, kinetic studies were performed, which revealed an even faster reaction compared to the previously used TBD, especially at low lignin loadings.

2. Results and Discussion

Lignin-PLA copolymers were synthesized from L-lactide and OrganoCat lignin using $[\text{Zn}\{(R,R)\text{-DMEG}_2(1,2)\text{ch}_2\}\text{OTf}_2 \text{ C1}]$ as

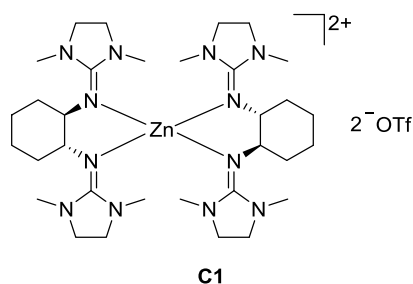


Figure 1. Molecular structure of $[\text{Zn}\{(R,R)\text{-DMEG}_2(1,2)\text{ch}_2\}\text{OTf}_2 \text{ C1}]$.^[21]

Table 1. Hydroxyl group content in OrganoCat lignin.

Type of OH ^{a)}	Aliphatic [mmol g ⁻¹]	Aromatic [mmol g ⁻¹]	Carboxylic [mmol g ⁻¹]	Total [mmol g ⁻¹]
	2.27 ± 0.03	4.36 ± 0.06	0.27 ± 0.01	6.91 ± 0.10

^{a)}calculated from $^{31}\text{P}\{^1\text{H}\}$ spectra of phosphitylated lignin after derivatization with TMDP. Aliphatic hydroxyl groups at 150.0–145.5 ppm. Aromatic hydroxyl groups at 144.0–137.6 ppm. Carboxylic hydroxyl groups at 136.0–134.4 ppm. Internal standard at 145.2 ppm. Phosphitylated water as reference at 132.2 ppm.^[74]

Table 2. Relative proportion of monomer units, bond types, and molecular weight data from OrganoCat lignin.

Relative proportion of monomer units ^{a)} [%]			Proportion of bond types ^{a)} [per 100 monomer units]			$M_n^b)$ [g mol ⁻¹]	$M_w^b)$ [g mol ⁻¹]	$\bar{D}^b)$ [–]
S-Type	G-Type	H-Type	$\beta\text{-O-4}$	$\beta\text{-5}$	$\beta\text{-}\beta$			
58	39	3	16	2	7	300 ± 50	2360 ± 30	8.5 ± 1.2

^{a)}Determined via HSQC NMR spectroscopy. Signal assignments were carried out according to the literature.^[77] ^{b)}Determined via SEC.

catalyst with lignin loadings ranging from 10 up to 50 wt% (Figure 1). The catalyst showed excellent activity in the polymerization of PLA homopolymers,^[21] and kinetic studies were conducted to investigate the effect of catalyst and lignin loading on the reaction. The resulting lignin-PLA copolymers were characterized by ^1H nuclear magnetic resonance (NMR) spectroscopy, ^{31}P NMR, diffusion-ordered spectroscopy (DOSY) NMR, 2D heteronuclear single-quantum correlation (HSQC) NMR, thermogravimetric analysis (TGA), and differential scanning calorimetry (DSC). After derivatization with the phosphitylation agent 2-chloro-4,4,5,5-tetramethyl-1,3,2-dioxaphospholane (TMDP), the influence of catalyst loading on the degree of lignin functionalization was investigated.

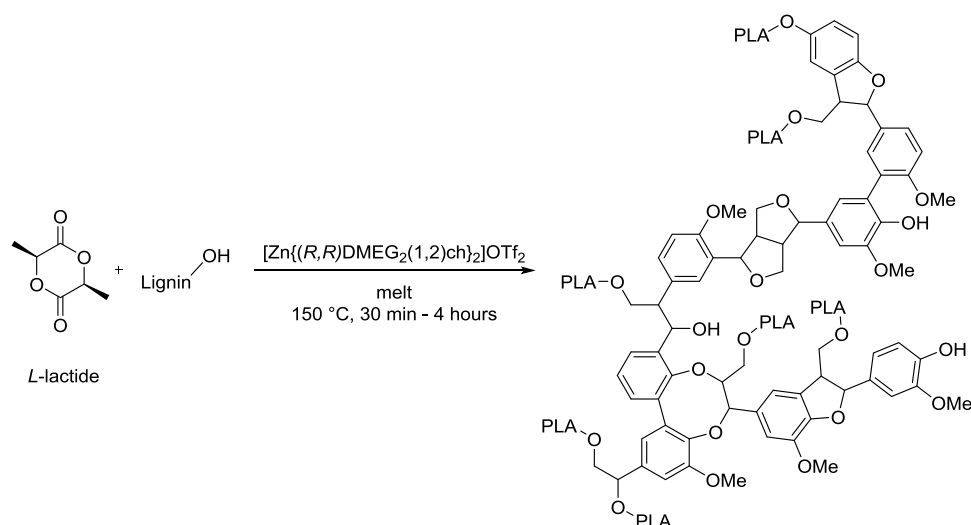
To quantify the number of hydroxyl groups of lignin, which act as reactive centers for functionalization, $^{31}\text{P}\{^1\text{H}\}$ NMR spectroscopy can be used.^[74] For this purpose, TMDP was added to lignin in the presence of pyridine, which leads to phosphitylation of hydroxyl groups. The integrals of the respective phosphitylated hydroxyl group can be compared with an internal standard, in this case phosphitylated cyclohexane (Table 1).

HSQC NMR spectroscopy is a powerful method to elucidate different structural characteristics of lignin and allows to quantify monomer units as well as binding types.^[75]

Analysis of the OrganoCat lignin shows primarily S-type monomer units as well as $\beta\text{-O-4}$ bonds as main linkage between monomer units (Table 2, Figure S35, Supporting Information). Additionally, size exclusion chromatography (SEC) has been carried out to determine the molecular masses of the OrganoCat lignin (Table 2, Figure S41, Supporting Information).

After resynthesis of complex C1,^[21] a series of lignin-PLA copolymers were prepared (Scheme 1). Both the lignin content and the lactide to catalyst ratios ($[\text{M}]/[\text{I}]$) were varied. The mass fractions of lignin ranged from 10 to 50 wt%, while the $[\text{M}]/[\text{I}]$ ratios were varied between 100:1 and 250:1. The structure of the copolymers is most likely star shaped, with a lignin core in the center and PLA chains as arms, which has been reported in the literature as well.^[66,71]

To verify the chemical linkage of the two species, DOSY NMR experiments were carried out (Figure S9–S16, Supporting Information). It was observed that the corresponding ^1H signals from the PLA chain and from lignin exhibit the same diffusion coefficient, which strongly supports the presence of a chemical linked copolymer. In order to exclude that PLA and lignin are present in an aggregated form, which would also result in a single diffusion coefficient, DOSY experiments were performed with pure lignin and PLA, and the mixture showed two different diffusion coefficients. (Figure S17, Supporting Information). The HSQC data of the resulting polymers show that the aromatic monomer units typical of lignin are retained. The corresponding peaks from the $\text{S}_{2/6}$ signal can be observed in all lignin-PLA



Scheme 1. Reaction scheme of the copolymerization of L-lactide with OrganoCat lignin.

copolymer samples at around $\delta_{1H} = 6.70$ and $\delta_{13C} = 103$ ppm. A signal for G-type monomers can be observed for G_5 at $\delta_{1H} = 6.67$ and $\delta_{13C} = 115$ ppm for most samples except at a lignin loading of 10 wt%. The reason for this is that the intensities in the aromatic region are not particularly pronounced, since the lignin concentration is too low in this case. Nevertheless, it can be concluded from these results that the lignin framework have been preserved during polymerization. (Figure S36–S40, Supporting Information)

First polymerization experiments were carried out with lignin loadings of 30% at $[M]/[I]$ ratios of 100:1 to gain first insights into the reaction system (Table 3, entry 1). The reaction proceeded in a reasonable time frame and a conversion of 89% was achieved after 2 h. Lowering the catalyst loading leads to a decrease of the reaction rate, which is the expected trend if the catalyst is the initiating species (Table 3, entry 2–4). The theoretical number average degree of polymerization ($DP_{n, \text{theo}}$) is not influenced by the $[M]/[I]$ ratio, because the concentration of hydroxyl groups in the lignin is much higher in comparison to the catalyst

loading. This can also be observed for the experimental number average degree of polymerization ($DP_{n, \text{exp}}$), which does not differ significantly with decreasing catalyst concentration. Also, $^{31}\text{P}\{^1\text{H}\}$ experiments show that the degree of functionalization of the polymers is not significantly affected with decreasing $[M]/[I]$ ratio resulting in uniform molecular masses and thus to uniform DP_n in the corresponding copolymers (Table S1, Supporting Information). Next, the lignin loading was varied from 10 up to 50 wt% (Table 3, entry 5–8). Decreasing the amount of lignin present in the reaction mixture leads to reduced reaction times and higher $DP_{n, \text{theo}}$. Notably, $DP_{n, \text{exp}}$ is roughly three times higher than $DP_{n, \text{theo}}$, which can be attributed to an incomplete activation of the hydroxyl groups at the lignin core. Less lignin in the reaction mixture leads to higher DP_n , which is an expected trend since lower hydroxyl group concentration in the reaction mixture would lead to fewer functionalization centers being present and therefore fewer PLA chains being started overall but reaching higher molecular masses. The $^{31}\text{P}\{^1\text{H}\}$ NMR spectroscopic analysis of the derivatized polymers showed a

Table 3. Copolymerization of L-lactide with OrganoCat lignin using C1.

	$[M]/[I]^a)$	lignin loading [wt%]	conversion ^{b)} [%]	time [min]	$k_{\text{app}}^c)$ [10^{-4} s^{-1}]	$DP_{n, \text{theo}}^d)$ [–]	$DP_{n, \text{exp}}^e)$ [–]
1	100:1	30	89	120	3.80	2	6 ± 1
2	150:1	30	86	150	2.31	2	5 ± 1
3	200:1	30	82	210	1.27	2	5 ± 1
4	250:1	30	81	270	1.15	2	5 ± 1
5	100:1	10	89	30	10.1	8	27 ± 4
6	100:1	20	95	60	6.12	4	12 ± 1
7	100:1	40	86	180	2.42	1	3 ± 1
8	100:1	50	80	150	2.12	1	2 ± 1
9	–	30	< 5	280	–	–	–

^{a)} $[LA]/[cat]$ ratio; ^{b)}Lactide conversion determined via ^1H NMR spectroscopy; ^{c)}Determined from the slope of the linear regression plotted from $\ln([LA]_0/[LA]_t)$ against time; ^{d)} $DP_{n, \text{theo}}$ by conversion $\times ([LA]/([OH]_{\text{lignin}} + [cat]))$; ^{e)}experimental $DP_{n, \text{exp}}$ calculated by $[I(\text{polymer})]/[I(\text{methine end group proton})]$, integrals were determined via ^1H NMR spectroscopy.

decrease in hydroxyl group concentration, which indicates an efficient initiation at the reactive centers. A higher hydroxyl group functionalization is observed for lower lignin loadings and the aliphatic hydroxyl groups are almost fully functionalized, while the aromatic and carboxylic hydroxyl groups remain partially unfunctionalized, which can be explained by the fact that the aliphatic hydroxyl groups exhibit increased reactivity for the ROP of lactide (Table S1, Supporting Information), which has already been shown in the literature for lactide^[65,66] as well as CL.^[59,61] It should be noted that even after longer reaction times the conversions did not rise significantly further, due to rising viscosity of the reaction mixture with increasing conversion. Control experiments without the addition of catalyst (Table 3, entry 9) confirmed that the catalyst is required to initiate the reaction and no autocatalysis occurs from the hydroxyl groups alone.

The lignin–PLA copolymer samples were analyzed via SEC (Figure S42, Supporting Information, Table 4). Due to the high polydispersity and nonuniformity of the initial lignin, the molecular mass distribution of the resulting copolymers is relatively broad and the determination of the absolute molecular masses is not straightforward. Nevertheless, it can be shown from the relative molecular weights that the molecular masses of the copolymers obtained is strongly dependent on the lignin content. With increasing lignin content, the molecular masses become smaller, as observed previously from the NMR data. The molecular masses are hardly affected by changing the catalyst concentration, although slightly higher values are obtained for $[M]/[I] = 100:1$ (Table 4, entry 1) than for lower catalyst loadings (Table 4, entry 2–4). The reason for this is on the one hand a higher lactide conversion and on the other hand this may be a statistical deviation resulting from the measurement uncertainty of the method. Nevertheless, the values are in a similar order of magnitude. The dispersities of the polymers differ slightly and not following any specific trend, which is most likely attributed to the high dispersity of the initial lignin and it can be concluded that neither the lignin content nor the catalyst concentration has a large effect on the width of the molecular mass distribution.

To investigate the reaction kinetics, aliquots were taken from the reaction mixture after appropriate time intervals and the conversion of the lactide was determined by ¹H NMR spectroscopy.

Table 4. SEC data of lignin–PLA copolymers.

	$[M]/[I]^a$	lignin loading [wt%]	M_n^b [g mol ⁻¹]	M_w^b [g mol ⁻¹]	\bar{D}^b [-]
1	100:1	30	3600	7300	2.0
2	150:1	30	1300	4300	3.4
3	200:1	30	1300	4300	3.4
4	250:1	30	1500	5500	3.8
5	100:1	10	5300	17 000	3.3
6	100:1	20	5600	12 000	2.2
7	100:1	40	1000	3800	2.9
8	100:1	50	700	1600	2.5

^a) $[LA]/[cat]$ ratio; ^b) Determined via SEC. Molecular masses are given relative to the polystyrene standard.

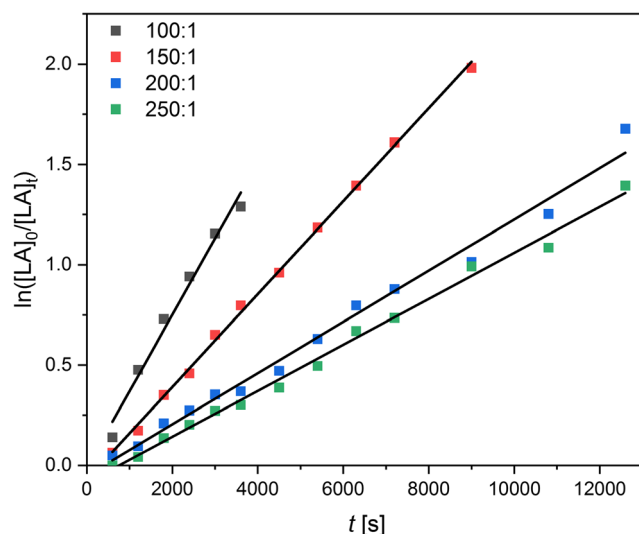


Figure 2. Semilogarithmic plots for the copolymerization of L-lactide and lignin loading of 30 wt% with varying $[M]/[I]$ ratios of 100:1 to 250:1 with respect to the lactide.

$\ln ([LA]_0/[LA]_t)$ was plotted against the time and the apparent polymerization rate constant k_{app} was determined from the slope of the linear regression (Figure 2). The linear regression was a suitable approximation for the plotted data, which indicates a controlled polymerization following the coordination insertion mechanism. Although higher catalyst loadings were used in this copolymerization, the apparent polymerization rate constants are about two orders of magnitude lower than the apparent polymerization rate constants from the PLA homopolymerization^[21] and the reaction proceeds overall in a slower manner (Table 3, entry 1–4). The introduction of lignin into the reaction system makes the reaction itself more complex and additional factors such as the accessibility of hydroxyl groups of lignin and catalyst transport can affect the rate of polymerization.

In order to investigate the influence of the lignin content on the reaction rate of the polymerization, copolymers with different lignin loadings were synthesized and the respective apparent polymerization rate constant k_{app} was determined as described above (Figure 3, Table 3, entry 5–8). The reaction proceeds in a faster manner, compared to TBD, which was used previously by Sattely et al., which reported reaction times between three and three and a half hours.^[65] Especially at lower lignin loadings, the reaction is significantly faster, and nearly full conversion is achieved after 30 min with lignin loadings of 10%. Interestingly, the reaction proceeds faster with low lignin loadings, despite the fact that less hydroxyl groups are present. This could be attributed to two effects. First, higher lignin loadings could lead to an increased viscosity of the reaction mixture, which influences the reaction rate significantly and lowers the catalyst accessibility. Second, higher lignin loadings could lead to faster catalyst deactivation, which would decrease the polymerization rate. Notably, the initiation of the polymerization seems to have an induction phase, especially at higher lignin loadings, where no conversion can be determined in the first few minutes. Another important fact which influences this behavior and needs

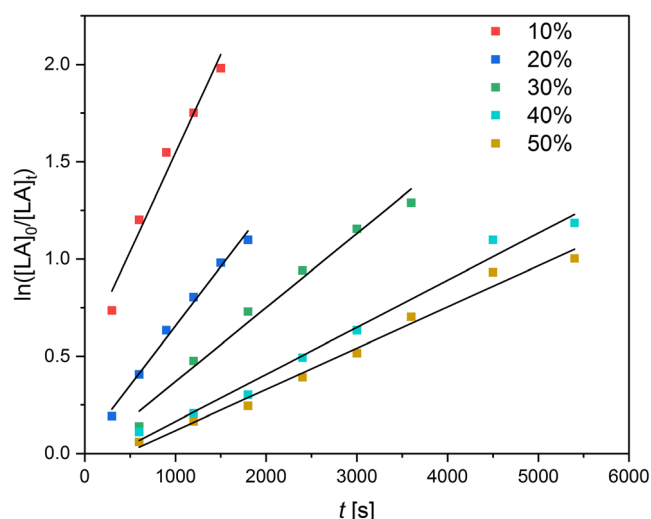


Figure 3. Semilogarithmic plots for the copolymerization of *L*-lactide and varying lignin loadings from 10 to 50 wt% with $[M]/[I]$ ratio of 100:1 with respect to the lactide.

to be considered is that the reaction mixture needs some time to melt homogeneously.

In comparison to PLA, lignin possesses a relatively high glass transition temperature T_g of 128 °C (Figure S33, Supporting Information), which is attributed to the rigid phenolic moieties and strong intermolecular hydrogen bonds in the lignin, which lead to relatively low thermal mobility. The glass transition temperature T_g as well as the melting temperature T_m of PLA depend on the tacticity of the polymer chain. Pure PLLA (PLA with *L*-lactide) has a T_g of 63 °C and a T_m of 178 °C.^[54] It is expected that the thermal properties are affected by the functionalization of the lignin core with PLA. DSC measurements revealed a T_g of 47 °C for a lignin loading of 10 %, where a higher lignin content leads to a higher T_g up to 92 °C for 50 wt% lignin (Table 5, Figure S28–S32, Supporting Information). Note that for higher lignin loadings (>30 wt%), the transition is relatively broad, similar to lignin, and the T_g are difficult to determine precisely. Thermal analysis via TGA revealed an increase in the average decay temperature with increasing lignin contents (Figure S34, Supporting Information).

Table 5. Glass transition temperatures of OrganoCat lignin and lignin–PLA copolymers with lignin loadings between 10 and 50 wt%.

Lignin loading [wt%]	Glass transition temperature T_g [°C] ^{a)}
10	47
20	48
30	53
40	77
50	92
Pure OrganoCat lignin	128

^{a)}determined via DSC.

3. Conclusion

Herein we could demonstrate an efficient way to synthesize star-shaped lignin–PLA copolymers with varying lignin ratios from 10 up to 50 wt% in a controlled manner using a zinc-based guanidine complex as catalyst. The reaction is carried out directly in the lactide melt and the PLA chains are grafted from the free hydroxyl groups of the lignin via ROP of the lactide. The molecular masses of each PLA chain attached to the lignin core is directly influenced by the lignin content of the polymer, with lower lignin content leading to higher molecular masses of the respective lactide chain. However, when the ratio of catalyst to lactide was varied, no significant effect on the molecular masses of the lactide chain was observed. $^{31}\text{P}\{^1\text{H}\}$ NMR experiments revealed that aliphatic hydroxyl groups were substituted preferably and the degree of functionalization at the lignin core is not significantly influenced by the catalyst loading. As expected, lower lignin loadings lead to higher functionalization of the lignin core. Interestingly, the reaction proceeds in a faster manner at lower lignin loadings, although less hydroxyl groups are present, which can be attributed to mass transportation limitations due to higher viscosity of the melt as well as catalyst deactivation processes at higher lignin loadings. Thermal analysis via DSC and TGA of the lignin–PLA polymers could show an increase in T_g and a higher thermal decomposition temperature with increasing lignin content. This study opens up new avenues to modified bioplastics which are not in competition with food and feed production.

4. Experimental Section

General Informations, Chemicals, and Methods: All reactions except the OrganoCat processing were performed under nitrogen atmosphere (99.996%), which was dried with P_4O_{10} using standard Schlenk techniques. All chemicals were purchased from Merck KGaA, abcr GmbH, Acros Organics, Th. Geyer GmbH & Co. KG, TCI Deutschland GmbH, VWR Deutschland GmbH, and Chemos GmbH & Co. KG and were used as received. Solvents were purchased in technical purity and distilled prior to use if needed. *L*-lactide was donated by Total Corbion PLA. TMDP^[76] and $[\text{Zn}\{(R,R)\text{-DMEG}_2(1,2)\text{ch}\}_2]\text{OTf}_2$ ^[21] were synthesized according to literature procedures. *L*-lactide was recrystallized once from hot toluene prior to use. Beech wood biomass was purchased from JRS as 0.75–2 mm particles (8% moisture) and used without further modification.

NMR spectra were recorded on a Bruker Avance II 400 or Bruker Avance III HD 400 nuclear resonance spectrometer operating at 400 MHz for ^1H and 162 MHz for ^{31}P . The signals were referenced to the residual proton signals of the deuterated solvent (CDCl_3 : $\delta(^1\text{H}) = 7.26$ ppm, DMSO: $\delta(^1\text{H}) = 2.50$ ppm, $\delta(^{13}\text{C}) = 39.52$ ppm). ^{31}P spectra were obtained as described in the literature and referenced to the reaction product of TMDP with water, giving a sharp signal at 132.2 ppm.^[52] DOSY NMR measurements were carried out using ^1H NMR standard processing applied on pseudo-2D datasets ($\text{si} = 8$ k, $\text{lb} = 0.3$, xf_2 , abs_2). HSQC NMR were measured with a Bruker standard pulse sequence “hscqgp” with 64 scans (7 h 20 min) measurement time. For the Bruker Avance III HD 400 the software Topspin (Version 3.5 pl 7) from Bruker and for the Bruker Avance II 400 the software TopSpin (Version 2.1) from Bruker were used for data acquisition. For visualization and examination of the NMR spectra, the software MestReNova (Version 12.0.1-20 560) from Mestrelab Research was used.

DSC curves of selected polymer samples were recorded on a Netzsch DSC 204 F1 Phoenix equipped with an intracooler. The samples were

weighed into 50 μ L aluminum pans and sealed with punctuated aluminum lids. For all measurements, three cycles were performed, starting at 20 °C and subsequent heating to 200 °C. After initial heating, an isotherm at 200 °C was applied for 15 min. A heating rate of 10 K min⁻¹ and a nitrogen flow of 40 mL min⁻¹ were applied. The analysis of data was performed with the software NETZSCH Proteus for Thermal Analysis Version 8.0.3.

TGA was carried out on a Mettler Toledo TGA (Greifensee, Switzerland) equipped with a compact cooling bath circulation thermostat Huber Ministat 125 (Offenburg, Germany). In a dynamic thermogravimetric method, 4.5 mg of sample was heated from 35 to 500 °C at a rate of 10 K min⁻¹ in an aluminum oxide pan and constant air flow of 50 mL min⁻¹. The evaluation of the results was carried out using the STARe V9.20 software.

The SEC analytics used for the molecular masses determination of OrganoCat lignin was a combination of high-performance liquid chromatography (HPLC) pump and autosampler (Agilent Technologies 1200 Series), a set of four SEC columns (1x precolumn PSS PolarSil in DMAc 50 \times 8 mm, 3x PSS PolarSil linear S in DMAc, 300 \times 8 mm) with a separation range of 100–300 000 Da. The columns were heated in an oven (Techlab K7) to 45 °C and analyzed by a refractive index detector (Wyatt Optilab rex) with a flow rate of 1 mL min⁻¹ with a sample concentration of 30 mg mL⁻¹. Lithium chloride was added to the eluent which was dimethylformamide (DMF) (UV/IR grade, Carl Roth, Karlsruhe Germany), so a 0.1 M solution was produced. For calibration, a polystyrene ReadyCal-Kit (PSS-PSKITR1L) set was used.

The molecular masses of lignin–PLA copolymers was determined using a Jasco-Ri-2031plus refractive index detector with a HPLC pump (Agilent 1260 Infinity) in combination with four MZ SDplus columns (50, 100, 1000, 10 000 Å) at 40 °C. Chloroform was used as a mobile phase with a flow rate of 1 mL min⁻¹. Relative molecular masses were obtained by conventional calibration with polystyrene standards.

General Procedure for Lignin Synthesis via OrganoCat Process: Lignocellulose fractionation was conducted as previously described with minor adaptations.^[45] In brief, 2.5 kg beech wood lignocellulose, 24.6 kg water, and 21.3 kg 2-MTHF were added into a 50 L stainless-steel high-pressure reactor. The reactor was closed and heated to 140 °C. Upon addition of 0.22 kg phosphoric acid (85 wt%), the mixture was stirred for 3 h at 140 °C. After cooling the reactor down to room temperature, the liquid phases were separated and lignin was precipitated from 2-MTHF in water.

General Procedure for the Phosphitylation of Lignin and Lignin–PLA Copolymers: Phosphitylation experiments were carried out according to a modified literature procedure.^[74] A solvent mixture of pyridine and deuterated chloroform (1.6:1; v/v) was prepared, stored under nitrogen, and protected from moisture with molecular sieves 3 Å. This solution was used to prepare a cyclohexanol solution (10.0 mg mL⁻¹) and a solution of chromium(III) acetylacetonate (5.0 mg mL⁻¹). Lignin or lignin–PLA copolymer (30 mg) were dissolved in pyridine/chloroform solution (0.6 mL). Subsequently, chromium(III) acetylacetonate solution (50 μ L) and cyclohexanol solution (50 μ L) were added to the dissolved sample. Finally, TMDP (75 μ L) was added the mixture. The mixture was allowed to stir for 1 h in the case of lignin or 24 h in the case of copolymer to ensure complete derivatization prior to ³¹P NMR analysis.

General Procedure for the Polymerization of L-Lactide with Lignin: In a nitrogen-filled glovebox, recrystallized L-lactide, lignin, and catalyst were weighed and thoroughly mixed in an agate mortar for 15 min. The homogeneous mixture was transferred into a 100 mL Schlenk flask and removed from the glovebox. The flask was equipped with an overhead stirrer, heated to 150 °C, and stirred at 150 rpm. After appropriate time periods, an aliquot was taken from the mixture, dissolved in deuterated dimethyl sulfoxide, and the lactide conversion was determined via ¹H NMR spectroscopy. After sufficient conversion was achieved, the reaction mixture was quenched by cooling under running water. The crude product mixture was dissolved in as little dichloromethane as possible (5–10 mL) and precipitated in excess diethyl ether at 0 °C. The polymer was washed with cold diethyl ether (2 \times 20 mL), ethanol (20 mL), and dried under reduced pressure in a vacuum oven at 60 °C. The lignin–PLA copolymers were obtained as a brown solid.

Supporting Information

Supporting Information is available from the Wiley Online Library or from the author.

Acknowledgements

The authors acknowledge the financial support of the Bioeconomy Science Center as part of the project LignoTex. The scientific activities of the Bioeconomy Science Center were financially supported by the Ministry of Innovation, Science and Research within the framework of the NRW Strategieprojekt BioSC (no. 313/323-400-002 13). The authors thank Total Corbion PLA for lactide donations. The authors thank Rainer Haas from the Institute of Technical and Macromolecular Chemistry at the RWTH Aachen University for SEC measurements of copolymer samples. The authors also thank RADAR4Chem for support and funding of the repository.

Conflict of Interest

The authors declare no conflict of interest.

Data Availability Statement

Original data of polymerization as well as NMR, TGA, DSC, and SEC data are available via the RADAR4Chem repository by FIZ Karlsruhe – Leibniz Institut für Informationsinfrastruktur and are published under an Open Access model (CC BY-NC-SA 4.0 Attribution-NonCommercial-Share Alike; DOI: <https://doi.org/10.22000/1740>). Open Access funding enabled and organized by Projekt DEAL.

Keywords

bioplastics, catalysis, copolymers, lignin, polylactides, renewable materials

Received: August 31, 2023

Revised: November 2, 2023

Published online:

- [1] R. Geyer, in *Mare Plasticum - The Plastic Sea*, Springer, Cham, Switzerland **2020**, Ch. 2, https://doi.org/10.1007/978-3-030-38945-1_2.
- [2] M. Gilbert, in *Brydson's Plastics Materials*, Butterworth-Heinemann, Oxford, United Kingdom **2017**, Ch. 1., <https://doi.org/10.1016/b978-0-323-35824-8.00001-3>.
- [3] A. L. Andrady, M. A. Neal, *Philos. Trans. R. Soc., B* **2009**, 364, 1977.
- [4] PlasticsEurope, *Plastics – the Facts 2022*, **2022**.
- [5] T. P. Haider, C. Volker, J. Kramm, K. Landfester, F. R. Wurm, *Angew. Chem., Int. Ed.* **2019**, 58, 50.
- [6] P. McKeown, M. D. Jones, *Sustainable Chem.* **2020**, 1, 1.
- [7] M. Fuchs, P. M. Schafer, W. Wagner, I. Krumm, M. Walbeck, R. Dietrich, A. Hoffmann, S. Herres-Pawlis, *ChemSusChem* **2023**, 16, e202300192.
- [8] A. Metz, A. Hoffmann, K. Hock, S. Herres-Pawlis, *Chem. Unserer Zeit* **2016**, 50, 316.
- [9] H. R. Kricheldorf, *Chemosphere* **2001**, 43, 49.
- [10] M. D. Jones, X. Wu, J. Chaudhuri, M. G. Davidson, M. J. Ellis, *Mater. Sci. Eng., C* **2017**, 80, 69.
- [11] P. M. Schafer, S. Herres-Pawlis, *ChemPlusChem* **2020**, 85, 1044.
- [12] A. B. Kremer, P. Mehrkhodavandi, *Coord. Chem. Rev.* **2019**, 380, 35.

- [13] L.-J. Wu, W. Lee, P. Kumar Ganta, Y.-L. Chang, Y.-C. Chang, H.-Y. Chen, *Coord. Chem. Rev.* **2023**, 475, 214847.
- [14] J. A. Stewart, P. McKeown, O. J. Driscoll, M. F. Mahon, B. D. Ward, M. D. Jones, *Macromolecules* **2019**, 52, 5977.
- [15] F. Chotard, R. Lapenta, A. Bolley, A. Trommschläger, C. Balan, J. Bayardon, R. Malacea-Kabbara, Q. Bonnin, E. Bodio, H. Cattey, P. Richard, S. Milione, A. Grassi, S. Dagorne, P. Le Gendre, *Organometallics* **2019**, 38, 4147.
- [16] P. McKeown, S. N. McCormick, M. F. Mahon, M. D. Jones, *Polym. Chem.* **2018**, 9, 5339.
- [17] H. Shere, P. McKeown, M. F. Mahon, M. D. Jones, *Eur. Polym. J.* **2019**, 114, 319.
- [18] J.-C. Buffet, J. Okuda, *Polym. Chem.* **2011**, 2, 2758.
- [19] C. Lackmann, J. Brendt, T. B. Seiler, A. Hermann, A. Metz, P. M. Schafer, S. Herres-Pawlis, H. Hollert, *J. Hazard. Mater.* **2021**, 416, 125889.
- [20] R. D. Rittinghaus, P. M. Schafer, P. Albrecht, C. Conrads, A. Hoffmann, A. N. Ksiazkiewicz, O. Bienemann, A. Pich, S. Herres-Pawlis, *ChemSusChem* **2019**, 12, 2161.
- [21] A. Hermann, S. Hill, A. Metz, J. Heck, A. Hoffmann, L. Hartmann, S. Herres-Pawlis, *Angew. Chem., Int. Ed.* **2020**, 59, 21778.
- [22] A. Hermann, T. Becker, M. A. Schafer, A. Hoffmann, S. Herres-Pawlis, *ChemSusChem* **2022**, 15, e202201075.
- [23] R. M. Rasal, A. V. Janorkar, D. E. Hirt, *Prog. Polym. Sci.* **2010**, 35, 338.
- [24] K. Stefaniak, A. Masek, *Materials* **2021**, 14, 5254.
- [25] J. Zhang, J. Xu, H. Wang, W. Jin, J. Li, *Mater. Sci. Eng., C* **2009**, 29, 889.
- [26] M.-J. Liu, S.-C. Chen, K.-K. Yang, Y.-Z. Wang, *RSC Adv.* **2015**, 5, 42162.
- [27] P. Gentile, V. Chiono, I. Carmagnola, P. V. Hatton, *Int. J. Mol. Sci.* **2014**, 15, 3640.
- [28] Y. Cheng, S. Deng, P. Chen, R. Ruan, *Front. Chem.* **2009**, 4, 259.
- [29] Y. Ramot, M. Haim-Zada, A. J. Domb, A. Nyska, *Adv. Drug Delivery Rev.* **2016**, 107, 153.
- [30] S. Farah, D. G. Anderson, R. Langer, *Adv. Drug Delivery Rev.* **2016**, 107, 367.
- [31] M. Puthumana, P. Santhana Gopala Krishnan, S. K. Nayak, *Int. J. Polym. Anal. Charact.* **2020**, 25, 634.
- [32] X. Pang, X. Zhuang, Z. Tang, X. Chen, *Biotechnol. J.* **2010**, 5, 1125.
- [33] S. Corneillie, M. Smet, *Polym. Chem.* **2015**, 6, 850.
- [34] S. Sen, S. Patil, D. S. Argyropoulos, *Green Chem.* **2015**, 17, 4862.
- [35] C. Wang, S. S. Kelley, R. A. Venditti, *ChemSusChem* **2016**, 9, 770.
- [36] A. Tribot, G. Amer, M. Abdou Alio, H. de Baynast, C. Delattre, A. Pons, J.-D. Mathias, J.-M. Callois, C. Vial, P. Michaud, C.-G. Dussap, *Eur. Polym. J.* **2019**, 112, 228.
- [37] D. S. Bajwa, G. Pourhashem, A. H. Ullah, S. G. Bajwa, *Ind. Crops Prod.* **2019**, 139, 111526.
- [38] F. Yue, F. Lu, R. C. Sun, J. Ralph, *J. Agric. Food Chem.* **2012**, 60, 922.
- [39] Y. Wang, J. Kalscheur, E. Ebikade, Q. Li, D. G. Vlachos, *J. Cheminformatics* **2022**, 14, 43.
- [40] J. Chen, X. Fan, L. Zhang, X. Chen, S. Sun, R. C. Sun, *ChemSusChem* **2020**, 13, 4356.
- [41] D. Weidener, M. Dama, S. K. Dietrich, B. Ohrem, M. Pauly, W. Leitner, P. Dominguez de Maria, P. M. Grande, H. Klose, *Biotechnol. Biofuels* **2020**, 13, 155.
- [42] A. Vishtal, A. Kraslawski, *Bioresour. Res.* **2011**, 6, 3547.
- [43] A. A. Maumun, M. A. Nikousaleh, M. Feldmann, A. Rüppel, V. Sauer, S. Kleinhans, H.-P. Heim, in *Lignin In Polymer Composites* (Eds: O. Faruk, M. Sain), William Andrew Publishing, Oxford, United Kingdom **2016**, Ch. 8, <https://doi.org/10.1016/B978-0-323-35565-0.00008-4>.
- [44] M. E. Eugenio, R. Martin-Sampedro, J. I. Santos, B. Wicklein, J. A. Martin, D. Ibarra, *Int. J. Biol. Macromol.* **2021**, 181, 99.
- [45] D. Weidener, W. Leitner, P. Dominguez de Maria, H. Klose, P. M. Grande, *ChemSusChem* **2021**, 14, 909.
- [46] T. vom Stein, P. M. Grande, H. Kayser, F. Sibilla, W. Leitner, P. Dominguez de Maria, *Green Chem.* **2011**, 13, 1772.
- [47] H. Liu, H. Chung, *J. Polym. Sci.* **2017**, 55, 3515.
- [48] H. Li, Y. Liang, P. Li, C. He, *J. Bioresour. Bioprod.* **2020**, 5, 163.
- [49] V. K. Ponnusamy, D. D. Nguyen, J. Dharmaraja, S. Shobana, J. R. Banu, R. G. Saratale, S. W. Chang, G. Kumar, *Bioresour. Technol.* **2019**, 271, 462.
- [50] B. Ahvazi, O. Wojciechowicz, T. M. Ton-That, J. Hawari, *J. Agric. Food Chem.* **2011**, 59, 10505.
- [51] S. S. Kelley, W. G. Glasser, T. C. Ward, *J. Wood Chem. Technol.* **1988**, 8, 341.
- [52] H. Sadeghifar, C. Cui, D. S. Argyropoulos, *Ind. Eng. Chem. Res.* **2012**, 51, 16713.
- [53] C. A. Cateto, M. F. Barreiro, A. E. Rodrigues, M. N. Belgacem, *Ind. Eng. Chem. Res.* **2009**, 48, 2583.
- [54] H. Nadj, C. Bruzzese, M. N. Belgacem, A. Benaboura, A. Gandini, *Macromol. Mater. Eng.* **2005**, 290, 1009.
- [55] Y. Li, A. J. Ragauskas, *J. Wood Chem. Technol.* **2012**, 32, 210.
- [56] W. G. Glasser, C. A. Barnett, T. G. Rials, V. P. Saraf, *J. Appl. Polym. Sci.* **1984**, 29, 1815.
- [57] T. Hatakeyama, Y. Izuta, S. Hirose, H. Hatakeyama, *Polymer* **2002**, 43, 1177.
- [58] S. Laurichesse, L. Avérous, *Polymer* **2013**, 54, 3882.
- [59] M. Li, Y. Pu, F. Chen, A. J. Ragauskas, *New Biotechnol.* **2021**, 60, 189.
- [60] W. de Oliveira, W. G. Glasser, *Macromolecules* **2002**, 35, 5.
- [61] J. Tian, Y. Yang, J. Song, *Int. J. Biol. Macromol.* **2019**, 141, 919.
- [62] I. K. Park, H. Sun, S. H. Kim, Y. Kim, G. E. Kim, Y. Lee, T. Kim, H. R. Choi, J. Suhr, J. D. Nam, *Sci. Rep.* **2019**, 9, 7033.
- [63] T. Hatakeyama, S. Yamashita, H. Hatakeyama, *J. Therm. Anal. Calorim.* **2019**, 143, 203.
- [64] M. Abdollahi, R. Bairami Habashi, M. Mohsenpour, *Ind. Crops Prod.* **2019**, 130, 547.
- [65] Y.-L. Chung, J. V. Olsson, R. J. Li, C. W. Frank, R. M. Waymouth, S. L. Billington, E. S. Sattely, *ACS Sustainable Chem. Eng.* **2013**, 1, 1231.
- [66] L.-E. Chile, S. J. Kaser, S. G. Hatzikiriakos, P. Mehrkhodavandi, *ACS Sustainable Chem. Eng.* **2018**, 6, 1650.
- [67] R. Liu, L. Dai, L. Q. Hu, W. Q. Zhou, C. L. Si, *Mater. Sci. Eng., C* **2017**, 80, 397.
- [68] W. Ren, X. Pan, G. Wang, W. Cheng, Y. Liu, *Green Chem.* **2016**, 18, 5008.
- [69] K. Dutta, A. Saikia, B. K. Saikia, A. Singh, *J. Polym. Environ.* **2023**, 31, 3393.
- [70] S. J. Kim, Y. S. Kim, O.-K. Lee, B.-J. Ahn, *Wood Sci. Technol.* **2016**, 50, 1293.
- [71] N. Zhang, M. Zhao, G. Liu, J. Wang, Y. Chen, Z. Zhang, *J. Mater. Sci.* **2022**, 57, 8687.
- [72] P. Ma, L. Jiang, P. Xu, W. Dong, M. Chen, P. J. Lemstra, *Biomacromolecules* **2015**, 16, 3723.
- [73] S. Y. Park, J.-Y. Kim, H. J. Youn, J. W. Choi, *Int. J. Biol. Macromol.* **2019**, 138, 1029.
- [74] A. Granata, D. S. Argyropoulos, *J. Agric. Food Chem.* **2002**, 43, 1538.
- [75] T. Q. Yuan, S. N. Sun, F. Xu, R. C. Sun, *J. Agric. Food Chem.* **2011**, 59, 10604.
- [76] P. Dais, A. Spyros, S. Christophoridou, E. Hatzakis, G. Fragaki, A. Agiomyrgianaki, E. Salivaras, G. Siragakis, D. Daskalaki, M. Tasioula-Margari, M. Brenes, *J. Agric. Food Chem.* **2007**, 55, 577.
- [77] K. Cheng, H. Sorek, H. Zimmermann, D. E. Wemmer, M. Pauly, *Anal. Chem.* **2013**, 85, 3213.